Triamidoamine Uranium(IV)-Arsenic Complexes Containing One-, Two-, and Three-fold U-As Bonding Interactions

Benedict M. Gardner,[1] Gábor Balázs,[2] Manfred Scheer,[2,*] Floriana Tuna,[3] Eric J. L. McInnes,[3] Jonathan McMaster,[1] William Lewis,[1] Alexander J. Blake,[1] and Stephen T. Liddle[1,*]

[1] School of Chemistry, University of Nottingham, University Park, Nottingham, NG7 2RD, UK.

[2] Institut of Inorganic Chemistry, University of Regensburg, Universitaets str.31, Regensburg, 93053, Germany.

[3] School of Chemistry and Photon Science Institute, University of Manchester, Oxford Road, Manchester, M13 9PL, UK.

*E-mail: stephen.liddle@nottingham.ac.uk; manfred.scheer@ur.de

Abstract

In order to further our fundamental understanding of the nature and extent of covalency in uranium-ligand bonding, and the benefits that this may have for the design of new ligands for nuclear waste separations, there is burgeoning interest in the nature of uranium complexes with soft- and multiple-bond-donor ligands. Despite this, there are no structurally authenticated examples of molecular uranium-arsenic bonds under ambient conditions. Here, we report structurally authenticated molecular uranium(IV)-arsenic bonds including formal single, double, and triple U-As bonding interactions. Compound formulations are supported by a range of characterization techniques, and theoretical calculations suggest the presence of polarized-covalent one-, two-, and three-fold bonding interactions between uranium and arsenic in parent arsenide [U-AsH$_2$], terminal arsinidene [U=AsH], and arsenido [U≡AsK$_2$] complexes, respectively. These studies inform our understanding of the bonding of actinides with soft donor ligands and may be of use in future ligand design in this area.

Introduction

Driven in part by a need for new extractants to separate, recycle, and reduce the volume of lanthanide and actinide spent-fission waste products in nuclear fuel cycles (*1*,*2*), there is burgeoning interest in probing the extent and nature of covalency in actinide-ligand chemical bonding (*3-7*). The most promising ligands for effecting such separations contain soft donor atom centers, e.g. nitrogen and sulfur, which has been attributed to the increased levels of covalency in actinide- compared to lanthanide-ligand bonds (*8-12*). If the performance of soft donor ligands is to be improved, and new classes are to be realized, then it is necessary to gain a better understanding of the nature and electronic structure of actinide-ligand bonding utilizing soft donors.

Uranium is one actinide that is amenable to routine study, and uranium-ligand multiple bond complexes have attracted attention because they would be expected to contain some covalency (*13-15*). Recently, in addition to numerous uranium-oxo derivatives, e.g. uranyl (*16*), there have been advances in the synthesis, characterization, and understanding of covalent, terminal uranium-carbene (*17-22*), -imido (*23-37*), -nitride (*38-40*), -phosphinidene (*41-43*), and heavier-chalcogenide (*44*,*45*) multiple bonds. Nevertheless, carbon, nitrogen, and oxygen donor ligands dominate, and post-first row donor ligands remain relatively rare, and sharply decrease in number as the periodic table is descended. For example, where pnictide donor ligands are concerned many uranium amido and imido complexes are known (*16*), but only two terminal uranium phosphinidene complexes (*42,43*) and four uranium and thorium polyphosphides are known (*46-49*). Indeed, given that uranium comes into contact with a wide range of elements in nuclear fuel cycles, it is surprising that there are no structurally authenticated molecular uranium-arsenic bonds of any type under ambient conditions (*50*,*51*). A thorium polyarsenide cluster is known (*52*), but otherwise uranium-arsenic complexes are limited to computational investigations (*53*) or low-temperature matrix isolation experiments (*54*,*55*).

Spurred on by prior matrix isolation experiments (*54*,*55*) and the recent isolation of terminal uranium(V) and (VI)-nitrides (*38*,*39*), we reported that by utilizing uranium(IV) precursors exemplified by [U(Tren^{TIPS})(THF)][BPh$_4$] [**1**, Tren^{TIPS} = N(CH$_2$CH$_2$NSiPr$^i_3$)$_3$], parent uranium(IV) pnictide complexes [U(Tren^{TIPS})(EH$_2$)] [E = N, **2a**; E = P, **2b**] can be accessed and converted to the corresponding uranium(IV) terminal parent imido and phosphinidene complexes [U(Tren^{TIPS})(EH)][K(L)$_2$] [E = N, L = 15-crown-5 ether (15C5), **3a**; E = P, L = benzo-15-crown-5 ether (B15C5), **3b**] (*37*,*43*). From a main group perspective, these species represent fundamental, metal-stabilized parent p-block fragments that are predominantly found as transient intermediates in the gas-phase or low-temperature matrices. The paucity of terminal parent EH (E = N, P) moieties can be traced back to the difficulty in kinetically stabilizing such naked fragments. Metal-ligand M=ER multiple bonds usually employ a sterically demanding R-group to help kinetically stabilize them. Thus, the isolation of EH or bare E is challenging where large metals, like uranium, are concerned. This is exemplified by **3a**, where the absence of a stabilizing R-group is apparent when **3a** is oxidized; disproportionation of the resulting uranium(V) imido derivative to tetravalent [U(Tren^{TIPS})(NH$_2$)] and hexavalent [U(Tren^{TIPS})(N)] occurs (*37*), but the bulkier uranium(V) imido complexes [U(Tren^{TIPS})(NR)] (R = adamantyl, SiMe$_3$) do not disproportionate (*39*).

With **2a**/**b** and **3a**/**b** in-hand, we turned our attention to whether the arsenic congeners could be isolated. Because the parent $(AsH_2)^-$ arsenide is sterically unhindered there are few examples of terminal M-AsH$_2$ linkages (*56*,*57*). The $(AsH)^{2-}$ arsinidene has been observed in the gas phase since the 1960s (*58*), but examples in the condensed phase are limited to μ_2- or μ_3-bridging modes to d-block metals to stabilize the charge accumulation at arsenic (*59*,*60*). Reports of a terminal M=AsH unit in the p-block are restricted to one example in an silylidenearsane/arsasilene with a HSi=AsH subunit (*61*). The $(As)^{3-}$ arsenido is rare in a molecular context, and only four terminal arsenidos with group 5 and 6 d-block metals are known (*62-64*). AsH$_n$ fragments are key intermediates in MOCVD materials processes so studying metal derivatives is germane to understanding their

properties. Although the covalent radius of arsenic is ca 0.1 Å larger than that of phosphorus, and the use of parent arsenic fragments would be envisaged to produce sterically unprotected, fragile linkages at uranium, we reasoned that **1** might still provide an effective entry to this chemistry.

Herein, we report structurally authenticated examples of molecular uranium(IV)-arsenic bonds including one-, two- and three-fold U-As bonding interactions; since the U-As bonds reported here are polarized and cannot be considered to be traditional, fully formed covalent single, double, and triple bonds, we adopt the nomenclature of one-, two-, and three-fold bonding interactions to indicate only that the arsenic centers donate one, two, or three electron pairs, respectively, to uranium.

Results

Synthesis and characterization. Addition of tetrahydrofuran to a cold (−78 °C) 1:1 mixture of **1** and [$KAsH_2$] (*65*) affords, after work-up, the parent uranium(IV) arsenide complex [$U(Tren^{TIPS})(AsH_2)$] (**2c**) in 54% yield as orange-brown blocks, Figure 1. The ^1H NMR spectrum of **2c** exhibits an AsH_2 resonance at −131.4 ppm, and the rest of the spectrum spans the range +11 to −39 ppm, which is consistent with the uranium(IV) formulation. The FTIR spectrum of **2c** exhibits As-H stretches at 2052 and 2031 cm^{-1}, respectively, which compares well to computed asymmetric and symmetric As-H stretches of 2080 and 2058 cm^{-1}, respectively, for the geometry optimized structure of **2c** (see below).

Since deprotonation of **2a**/**2b** gives **3a**/**3b**, and a similar method yielded a terminal molybdenum carbide (*66*), we examined the deprotonation of **2c**. Treatment of **2c** with one equivalent of benzyl potassium in cold (−78 °C) toluene affords, after work-up, a dark brown sticky solid putatively formulated as [$U(Tren^{TIPS})${AsH(K)}]; this has resisted all attempts at isolation, but addition of hexane to a cold (−78 °C) mixture of it and two equivalents of B15C5 affords, after work-up, black

crystals of the uranium(IV) arsinidene complex [U(Tren^{TIPS})(AsH)][K(B15C5)$_2$] (**3c**) in 24% yield, Figure 1. The ^{1}H NMR spectrum of **3c** spans the range +7 to −27 ppm, which is a similar range to the majority of resonances for **2c** consistent with the presence of uranium(IV). The AsH hydrogen atom could not be observed in the ^{1}H NMR spectrum, analogously to **3b** where the PH hydrogen atom resonance was not observed (*43*). This is attributed to line-broadening arising from the close proximity of the AsH hydrogen atom to the paramagnetic uranium(IV) ion. The FTIR spectrum of **3c** exhibits a weak As-H stretch at 1857 cm^{-1}, which compares well to a computed As-H stretch of 1831 cm^{-1} for the geometry optimized structure of **3c** (see below).

Since mono-deprotonation of **2c** to give **3c** had been effected, we were interested to determine whether the remaining arsinidene hydrogen atom could be removed to yield an arsenido complex. Treatment of **2c** with two equivalents of benzyl potassium in cold (−78 °C) toluene affords an intense dark yellow solution; concentration of the solution affords dark brown crystals of the uranium(IV) arsenido complex [{U(Tren^{TIPS})(AsK$_2$)}$_4$] (**4**) in 50% yield, Figure 1. Reflecting its tetrameric formulation (see below), the ^{1}H NMR spectrum of **4** exhibits a single broad resonance (fwhm = ~1500 Hz). The FTIR spectrum is consistent with removal of all arsenic-bound hydrogen atoms since it is devoid of absorptions in the As-H stretch region.

With **4** in hand we attempted to abstract the potassium ions. Addition of 12-crown-4, 15C5, or B15C5 (8 or 16 equivalents per tetramer), or 18-crown-6 or dibenzo-18-crown-6 (4 or 8 equivalents per tetramer) ethers to abstract one or both potassium ions per arsenic center resulted in intractable mixtures. However, treatment of **4** with 4 molar equivalents of 2,2,2-cryptand resulted in isolation of the uranium(IV) arsinidiide complex [U(Tren^{TIPS})(AsH)K(2,2,2-cryptand)] (**5**). In an attempt to combine uranium oxidation and potassium abstraction into one step, **4** was treated with AgBPh$_4$, but this resulted in the formation of intractable mixtures. When oxidation was attempted with PbI$_2$, only the uranium(IV) cyclometallate [U{N(CH$_2$CH$_2$NSiPr$^i_3$)$_2$(CH$_2$CH$_2$NSiPr$^i_2$CHMeCH$_2$)}] (**6**)

could be isolated (*67*). We note that if the synthesis of **3c** is not limited to two hours and is stirred for two days the diuranium(IV) triarsenide complex [{U(Tren^{TIPS})}$_2$(μ:η^3-η^3-As$_3$)][K(B15C5)$_2$] (**7**) is the only isolable product. Both **5** and **7** could only be isolated in very low yields (2 and <1%, respectively) and so are only partially characterized (See the Supplementary Information, Methods).

Solid state structures. In order to confirm the formulations of **2c**, **3c**, and **4** we determined their solid state structures by X-ray crystallography, Figure 2 (the structures of **5** and **7** can be found in the Supplementary Information Figures S1 and S2). Complex **2c** exhibits a terminal AsH_2 unit residing *trans* to the Tren-amine center [N3-U1-As1 ∠ = 177.3(10°]. The U1-As1 bond length of 3.004(4) Å is slightly longer than the sum of the single bond covalent radii for uranium and arsenic (2.91 Å) (*68*); there are no other U-As bond lengths for comparison, but it can be compared to the uranium(IV)-phosphorus distance of 2.883(2) Å in **2b** (*43*), where the difference can almost entirely be ascribed to the larger covalent radius of arsenic compared to phosphorus. The uranium(IV)-amide distances [average 2.20(4) Å] and uranium(IV)-amine distance of 2.67(3) Å are typical of uranium(IV)-Tren complexes. The U1-As1-H bond angles average 94.75°, reflecting the high degree of p-character in post-first row main group element-element covalent bonds.

The structure of **3c** confirms the separated ion pair formulation and that the arsinidene is terminal and *trans* to the Tren^{TIPS} amine center [N4-U1-As1 ∠ = 177.70(16)°]. The U1-As1 bond length of 2.7159(13) Å is ca 0.29 Å (9.6%) shorter than the uranium(IV)-arsenic bond in **2c**, but ca 0.24 Å longer than the sum of the double bond covalent radii for uranium and arsenic (2.48 Å) (*69*). This can be attributed to the anionic, electron-rich formulation of the [U(Tren^{TIPS})(AsH)]$^-$ fragment and the sterically demanding nature of Tren^{TIPS} combined with a large arsenic center. The anionic nature of the uranium(IV)-containing portion of **3c** is also reflected in the U-N$_{amide}$ and U-N$_{amine}$ distances of 2.310(7) (av.) and 2.690(7) Å, respectively, which are long for uranium(IV)-Tren U-N distances. The U1-As1-H1 bond angle is 90(6)°.

In the solid state tetrameric **4** is composed of an As_4K_6 adamantane-type core which contains an interstitial potassium ion. The last potassium ion is grafted onto one face of the core to give an $\{As_4K_8\}^{4-}$ polyhedron. Each arsenic center then coordinates to a $[U(Tren^{TIPS})]^+$ fragment to give the neutral cluster. The U-As bond lengths average 2.7511(19) Å [range: 2.730(2)-2.775(2) Å], which is longer than would be expected from the sum of the covalent triple bond radii of uranium and arsenic (2.24 Å) (*70*) but still 8.4% contracted compared to the U-As bond distance in **2c**. Thus, although the remaining arsenic-bound hydrogen atom has been removed, in principle allowing a three-fold U-As bonding interaction, this bond is attenuated by coordination to multiple potassium ions; as a result the U-As bond lengths in **4** are ca 0.03 Å longer than the formal U=As double bonding interaction in **3c**. However, some steric buttressing may also be operating because it is germane to note that like anionic **3c** the average $U\text{-}N_{amide}$ and $U\text{-}N_{amine}$ bond distances in neutral **4** are long at 2.313(19) (av.) and 2.758(13) Å, respectively; it is also notable that the normally planar Tren-amides are pyramidalized to varying extents, to give pseudo-C_3 symmetric propeller-shaped Tren ligands rather than the usual pseudo-C_{3v} symmetric conformer, which suggests steric saturation. The As-K distances are long [range: 3.107(15)-3.847(12) Å] compared to the sum of the covalent single bond radii of arsenic and potassium (3.17 Å) (*68*), which implies electrostatic bonding. Three of the arsenic centers adopt distorted octahedral geometries, whereas the fourth arsenic center is a distorted trigonal bipyramid; in each case the distortions arise from the equatorial potassium ions being displaced away from the $[U(Tren^{TIPS})]$ component towards the $\{As_4K_8\}^{4-}$ core.

Magnetic and electronic absorption studies. The variable temperature magnetic moment behaviors for **2c**, **3c** and **4** in the solid-state are similar (Figure 3; see Supplementary Figures S3-S5 for magnetic susceptibility plots). The room temperature values of **2c**, **3c** and **4** are 2.79, 2.67 and 5.63 μ_B (the latter value corresponds to 2.82 μ_B per uranium ion), respectively, and agree well with Evans method solution values of 2.93, 2.75 and 2.75 μ_B (per uranium ion). On cooling, the

magnetic moments decrease steadily in each case, reaching 1.00, 0.87 and 2.65 μ_B (1.33 μ_B per U ion), respectively, at 1.8 K and tending towards zero in each case. These data are consistent with the uranium(IV) formulations, since the lowest energy component of the $^3H_4$ ground term is a magnetic singlet (*71*). To further confirm the tetravalent formulations of **2c**, **3c** and **4** we examined their electronic absorption spectra in the range 5,000-25,000 cm^{-1} (See the Supplementary Information Figures S6 and S7), and the data are consistent with the uranium(IV) formulations.

Computational studies. In order to probe the nature of the uranium(IV)-arsenic linkages in **2c** and **3c** we conducted density functional theory (DFT) calculations on the full structure of **2c** and the anion component of **3c**. The calculated bond lengths and angles are within 0.05 Å and 2° of the experimentally determined structures. The size of **4** rendered geometry optimization intractable; however, we were able to conduct a single point energy calculation on a simplified model of **4** (**4'**) using crystal structure coordinates where the *iso*-propyl groups were replaced by hydrides. In all cases the calculations can be considered to present qualitative descriptions of the electronic structures of **2c**, **3c**, and **4**, Table 1.

The calculated uranium MDC-q charges (2.42-2.74) are typical of Tren-uranium(IV) complexes (*37*,*43*). The calculated arsenic MDC-q charges reflect the changes from formally mono-anionic arsenide (−0.51) to dianionic arsinidene (−0.89) to trianionic arsenido (av. −1.77) in **2c**, **3c**, and **4'**, respectively. The calculated uranium MDC-m spin densities span the range 2.25-2.52 and, together with the calculated charges support the notion of increased donation of electron density from the arsenic ligands to uranium in the order **4'** > **3c** > **2c** as would be expected. The calculated U-As Mayer bond orders of 0.69 and 1.62 in **2c** and **3c**, respectively, are consistent with polarized-covalent U-As single and U=As double bonding interactions in terminal arsenide and arsinidene complexes. For comparison, the U-N_{amide} and -N_{amine} Mayer bond orders average 0.67 and 0.30, respectively. The situation for **4'** is more complex. Specifically, the five-coordinate arsenido center

exhibits the shortest U-As distance and the highest Mayer bond order (1.75). The other three six-coordinate arsenido centers exhibit progressively longer U-As distances with correspondingly decreasing Mayer bond orders (1.48-1.38). Notably, as the U-As bond lengthens the uranium(IV) centers become less electron-rich as evidenced by the calculated MDC-q and -m charges and spin densities, respectively. The calculated U-As Mayer bond orders in **4'** reflect the presence of coordinated potassium ions. For comparison, the As-K Mayer bond orders are calculated to be ca 0.1 (av.), as expected for electrostatic interactions.

Inspection of the Kohn Sham frontier orbitals of **2c**, **3c**, and **4'** (See Supplementary Information Figures S8-S11) reveal that the uranium(IV)-arsenic interactions are dominated by arsenic 4p-orbitals and uranium 5f-orbitals. Consistent with their uranium(IV) formulations, the HOMO and HOMO−1 (for **2c** and **3c**) and HOMO to HOMO−7 (for **4'**) are singularly-occupied α-spin orbitals of essentially pure 5f-character. The latter grouping spans a narrow range of 0.16 eV, commensurate with their essentially non-bonding nature. The following uranium-arsenic molecular orbitals have α- and β-spin counterparts that are occupied. Within the α-spin manifold, the HOMO−2 of **2c** represents the principal uranium(IV)-arsenide interaction and is predominantly a 4p orbital that constitutes the U-As σ-bond and a pseudo lone pair. In **3c**, the HOMO−2 and −3 orbitals represent the principal components of the uranium(IV)-arsinidene double bond, with the former being of π-symmetry, lying ~0.12 eV higher in energy than the latter which is the σ-bonding interaction. For **4'**, the four uranium(IV)-arsenido σ- and eight π-bonding interactions are combined into a densely packed manifold (0.65 eV range) spanning HOMOs −8 to −19. Because of the narrow energy range and mixing of the twelve U-As bonding combinations the σ/π energy ordering remains uncertain, which is debatable since in terminal uranium(V) and (VI)-nitrides the U≡N σ-interactions are calculated to lie higher in energy than the π-interactions (*38*,*39*).

Consistent with the DFT calculations, natural bond orbital (NBO) analyses of **2c**, **3c**, and **4'** return

one σ^2, one $\sigma^2\pi^2$, and four $\sigma^2\pi^4$ U-As interactions, respectively, and confirms that all the arsenic interactions with uranium are mediated via arsenic orbitals of essentially pure 4p-character, Figures 4 and 5 and Table 1. For **2c**, the σ-bond is composed of 13.3 and 86.7% uranium and arsenic character, respectively and the uranium component exhibits a 5f:6d split of 48:47% (7s + 7p = 5%). For **3c**, the σ-bond is composed of 11.2% uranium and 88.8% arsenic character, whereas the π-bond is 12.7 and 87.3% uranium and arsenic character, respectively; with the establishment of a U=As double bonding interaction, the calculations suggest that 5f-character now dominates the uranium bonding component. For the σ-bond the uranium 5f:6d contribution is composed 61:37 and the π-bond comprises 66:33% character with the remainder of each made up of modest 7s or 7p contributions (<2%). The bonding interactions in **4'** vary due to the different arsenic coordination modes, but it is notable that the five-coordinate arsenido-uranium(IV) bond exhibits the largest uranium contributions. Specifically, the σ-bond is composed of 17.1% uranium and 82.9% arsenic character, whereas the two π-bonds are composed of 19.2/16.2% and 80.8/83.8% uranium and arsenic character, respectively. The 5f:6d ratio in the uranium components vary considerably, being 57:40 for the σ-bond, and 69:30/55:44 for the two π-bonds, with the remainder being 7s or 7p character (<3%). For the three six-coordinate arsenido-uranium(IV) linkages, the uranium contributions for the σ- and π-bonds vary from 13.1 to 15.7% and 12.1 to 14.2%, respectively. Here, the 5f contributions dominate over 6d more consistently, ranging from 54:45% to 73:24% with modest contributions from 7s and 7p (<4%).

We examined the topologies of the U-As linkages in **2c**, **3c**, and **4'** using the Atoms in Molecules approach to analyse the topological electron density [$\rho(\mathbf{r})$], the Laplacian of the electron density [$\nabla^2\rho(\mathbf{r})$], and the bond ellipticity parameters [$\varepsilon(\mathbf{r})$]. For each U-As interaction a 3,-1 bond critical point (BCP) was identified. The [$\rho(\mathbf{r})$] values for **2c**, **3c**, and **4'** are in the range ~0.04-0.07, which suggests electrostatic bonding with modest covalent contributions; covalent bonds tend to exhibit calculated [$\rho(\mathbf{r})$] values >0.2, though whether this convention, formulated for lighter elements, is

applicable for uranium is debateable. The [$\nabla^2\rho(\mathbf{r})$] terms span the range ~0.02-0.05 for **2c**, **3c**, and **4'**, and are all positive as tends to be the case with bonds involving post-first row elements since the positive λ_3 curvature term outweighs the negative λ_1 and λ_2 values beyond first row elements. In agreement with the DFT and NBO analyses, the [$\varepsilon(\mathbf{r})$] values of 0.09, 0.39, and 0.02 (av.) confirm the presence of polarized single, double, and triple U-As bonding interactions in **2c**, **3c**, and **4'**; for a cylindrical σ-bond the ellipticity is 0, a bond with only one π-contribution has an ellipticity > 0, whereas a bond with two π-components returns to an ellipticity of 0 (*72*).

Discussion

The synthesis of complex **2c** can be accomplished when **1** is used, whereas use of [U(Tren^{TIPS})(X)] (X = Cl or I) fails, which can be rationalized on hard-soft acid-base grounds since arsenic is a soft base and uranium(IV) is a hard acid. Fine-grinding of the [$KAsH_2$] and a short reaction time of thirty minutes are essential for obtaining good yields of **2c**. When the [$KAsH_2$] is not well-ground the reaction is sluggish and yields decrease dramatically on extended reaction times. It is unusual for the sterically unencumbered AsH_2 to bind in a terminal bonding mode (*56*,*57*), which reflects the sterically demanding nature of Tren^{TIPS}.

The facile deprotonation of **2c** to give **3c** is noteworthy, since although this is established chemistry for **2a** and **2b**, for **2c** the arsenide hydrogens may exhibit hydridic character, yet are straightforwardly removed, formally, as protons. Additionally, the U-As bond would be predicted to be weak and vulnerable to facile dissociation; indeed, the reaction time must be kept to around two hours since longer reaction times result in decomposition and only **7** can be recovered. Complex **3c**, as a metal-stabilized terminal parent arsinidene complex, has no precedent; examples in the condensed phase are rare and usually involve μ_2- or μ_3-AsH bridging modes to d-block metals (*59*,*60*) because of its sterically unencumbered nature and to stabilize the formal charge

accumulation at arsenic. Reports of a terminal M=AsH unit are restricted to one example in the p-block in an arsasilene complex with a HSi=AsH subunit (*61*).

More surprising than the mono-deprotonation of **2c** is that double deprotonation can be effected to access the arsenido complex **4**, adding to a class of metal-ligand multiple bond previously limited to the d-block (*62-64*). Uranium(IV) generally forms more polarized multiple bonds with ligands than uranium(V) or (VI), so any uranium(IV)-ligand multiple bond would be expected to be reactive and weak. The potassium ions in tetrameric **4** clearly play an important role in stabilizing charge localization at the arsenido centers because when they are removed the arsenido centers abstract protons from solvent to form the arsinidiide complex **5**. The vulnerability of the uranium-arsenic bonds in **4** is also underscored by the isolation of **6**. Although the intention of simultaneous potassium abstraction and uranium(IV) oxidation, by treating **4** with $AgBPh_4$ or PbI_2, was to provide a more stabilized U≡As three-fold bonding interaction, by way of a higher oxidation state of uranium to offset the removal of stabilizing potassium cations, it is clearly not a sufficient stabilization, as evidenced by formation of the cyclometallate complex **6** or intractable product mixtures. Although isolated from the decomposition of **3c** in low yield, **7** permits a glimpse into the complex chemistry, including catenation, that is clearly operating, and it is notable for being an isolobal analogue of a bridging cyclopropylidene diuranium(IV) complex, which is yet to be reported. These results show that the U-As linkage is fragile and a supporting ligand larger than $Tren^{TIPS}$ may be required to isolate a terminal U≡As bond under ambient conditions.

Regarding the magnetic data for **2c**, **3c**, and **4**, the rate of decrease of the magnetic moment for **4** (per uranium ion) on cooling is notably slower below ~50 K than for **2c** or **3c**, which implies that the lowest paramagnetic excited states are lower lying in **4**. Therefore, these states in **4** are thermally accessible even at low temperature, but in turn the higher lying states are well isolated so the magnetic moment rises slowly >50 K. This is also consistent with the fact that the lowest

temperature magnetic moment of **4** (per uranium ion) is greater than **2c** or **3c**. Similar behaviour has been observed for uranium-fluorides compared to other halides, which is rationalized on the basis of a strong point charge giving a strong crystal field (*73*). Thus, the data suggest that **4** has the strongest point charge and crystal field, compared to **2c** and **3c**, which is consistent with its formally $(As)^{3-}$ nature. The magnetic moments for the U=EH **3a-c** series at the lowest measured temperature (2 K) are ordered N > P > As (1.50, 1.04, and 0.87 μ_B) (*37*,*43*), which shows that the imido enforces the strongest ligand field at uranium(IV) and the arsinidene the least. When comparing the U-EH_2 **2a-c** and U=EH **3a-c** series, **3a**/**b** (E = N, P) exhibit higher low temperature magnetic moments than for their **2a**/**b** analogues, respectively, which is consistent with the stronger donating power of the pnictide centers and thus stronger crystal fields/point charges in **3a**/**b** compared to **2a**/**b**; however, **3c** is very similar to **2c**, perhaps reflecting the polarized nature of the U-As bonds and weak donor strength of arsenic.

Computational analyses of the uranium(IV)-arsenic bonds in **2c**, **3c**, and **4'**, consistently suggest σ^2, $\sigma^2\pi^2$, and $\sigma^2\pi^4$ bonding interactions, respectively. Uranium(IV) utilizes variable levels of 5f and 6d orbital mixing in bonding to arsenic, ranging from ~50:50 to ~75:25, normalized after removal of 7s and 7p contributions (~4% total); however it is clear that 5f-orbitals dominate the uranium(IV) bonding overall. The uranium(IV)-arsenic bonds in **2c**, **3c**, and **4'** are clearly polarized, and thus even though one-, two-, and three-fold electron-pair bonding interactions, respectively, can be clearly identified, this results in Mayer bond orders that deviate below the hypothetical bond orders of 1, 2, and 3, respectively. This is also evidenced in **3a** where a three-fold bonding interaction in the U=NH bond has a Mayer bond order of only 1.75 (*37*). The bond topology analysis suggests that the U-As bonds are polarized, and in agreement with DFT and NBO analyses confirms the presence of σ^2, $\sigma^2\pi^2$, and $\sigma^2\pi^4$ U-As bonding interactions in **2c**, **3c**, and **4'**. Although it should be recognised that dipolar U^{n+}-As^{n-} resonance forms will contribute to the electronic structure of these U-As linkages, the ellipticity values for σ^2 **2c** and $\sigma^2\pi^4$ **4'** are similar to that of ethane (0.0) and

acetylene (0.0), whereas that of **3c** lies between those of benzene (0.23) and ethylene (0.45) and exceeds the calculated value for the parent *E*-diarsene HAs=AsH (0.33) (*63,74*).

Summary and Conclusions

In summary, we report structurally authenticated molecular uranium-arsenic bonds including one-, two-, and three-fold bonding interactions. These studies show that the U-As bond is fragile, but with a suitable sterically demanding supporting ligand like $Tren^{TIPS}$ these bond linkages can be stabilized. Computational analyses suggest that σ^2, $\sigma^2\pi^2$, and $\sigma^2\pi^4$ U-As bonding interactions are present in **2c**, **3c**, and **4**, respectively, but also suggest that these linkages are polarized. Magnetic studies provide qualitative bracketing of the relative crystal field strengths of arsenide, arsinidene, and arsenido ligands, and support the notion that the arsenido ligand in **4** exhibits the strongest point charge and crystal field at uranium(IV) compared to **2c** and **3c**, which are similar to each other, perhaps reflecting the polar nature of these U-As bonds. As in related nitride complexes (*38*,*39*) calculations suggest that uranium tends to deploy 5f orbitals more than 6d orbitals in the U-As bonds (*74*). The complexes reported herein add to our understanding of actinide-ligand multiple bonds and soft uranium-ligand combinations more broadly and may in the future inform the design of new soft-donor ligands for the actinides.

Methods

General. Experiments were carried out under a dry, oxygen-free dinitrogen atmosphere using Schlenk-line and glove-box techniques. All solvents and reagents were rigorously dried and deoxygenated before use. Compounds were variously characterized by elemental analyses, NMR, FTIR, and UV/Vis/NIR electronic absorption spectroscopies, Evans and SQUID magnetometric methods, single crystal X-ray diffraction studies, and DFT, NBO, and bond topology theoretical calculations. Further details are available in the Supplementary Information. The arsenic-bound hydrogen atoms in **2c** and **3c** were initially located in the Fourier transform difference maps and

refined with geometric restraints based on literature data and metrical data computed from the DFT geometry optimizations. The crystal structures of **2c** and **4** suffered from weak diffraction and consequently the data are poor, but the chemical connectivities of all the compounds reported here are beyond reasonable doubt.

Accession codes

The X-ray crystallographic coordinates for structures reported in this Article have been deposited at the Cambridge Crystallographic Data Centre (CCDC), under deposition number CCDC 1045599 and 1045600 (two data sets) (**2c**), 1045601 (**3c**), 1045602 (**4**), 1045603 (**5**), and 1045604 (**7**). These data can be obtained free of charge from The Cambridge Crystallographic Data Centre via www.ccdc.cam.ac.uk/data_request/cif.

Acknowledgments

We thank the Royal Society, the European Research Council, the Engineering and Physical Sciences Research Council, the Universities of Nottingham, Manchester, and Regensburg, the Deutsche Forschungsgemeinschaft, the UK National Nuclear Laboratory, COST Action CM1006, and the EPSRC UK National EPR Facility for generously supporting this work.

Supplementary Information

Accompanies this paper at…

Author Contributions

B.M.G. synthesized and characterized the compounds. G. B. prepared the parent potassium arsenide complex. F.T. and E.J.L.M. recorded and interpreted the magnetic data. J.M. and S.T.L. conducted and analyzed the theoretical calculations. W.L. and A.J.B. carried out the X-ray single crystal diffraction work. S.T.L. and M.S. originated the central idea, supervised the work, analyzed the data

and wrote the manuscript with contributions from all the co-authors.

References

1. Dam, H. H., Reinhoudt, D. N. & Verboom, W. Multicoordinate ligands for actinide/lanthanide separations. *Chem. Soc. Rev.* **36**, 367-377 (2007).
2. Jones, M. B. & Gaunt, A. J. Recent developments in synthesis and structural chemistry of nonaqueous actinide complexes. *Chem. Rev.* **113**, 1137-1198 (2013).
3. Kozimor, S. A. *et al.* Trends in covalency for d- and f-element metallocene dichlorides identified using chlorine K-edge X-ray absorption spectroscopy and time-dependent density functional theory. *J. Am. Chem. Soc.* **131**, 12125-12136 (2009).
4. Seaman, L. A. *et al.* Probing the 5f orbital contribution to the bonding in a U(V) ketimide complex. *J. Am. Chem. Soc.* **134**, 4931-4940 (2012).
5. Minasian, S. G. *et al.* Determining relative f and d orbital contributions to M-Cl covalency in MCl_6^{2-} (M = Ti, Zr, Hf, U) and $UOCl_5^-$ using Cl K-edge X-ray absorption spectroscopy and time-dependent density functional theory. *J. Am. Chem. Soc.* **134**, 5586-5597 (2012).
6. Spencer, L. P. *et al.* Tetrahalide complexes of the $[U(NR)_2]^{2+}$ ion: synthesis, theory, and chlorine K-edge X-ray absorption spectroscopy. *J. Am. Chem. Soc.* **135**, 2279-2290 (2013).
7. Lukens, W. W. *et al.* Quantifying the σ and π interactions between U(V) f orbitals and halide, alkyl, alkoxide, amide, and ketimide ligands. *J. Am. Chem. Soc.* **135**, 10742-10754 (2013).
8. Jensen, M. P. & Bond, A. H. Comparison of covalency in the complexes of trivalent actinide and lanthanide cations. *J. Am. Chem. Soc.* **124**, 9870-9877 (2002).
9. Miguirditchian, M. *et al.* Thermodynamic study of the complexation of trivalent actinide and lanthanide cations by ADPTZ, a tridentate N-donor ligand. *Inorg. Chem.* **44**, 1404-1412 (2005).

10. Gaunt, A. J. *et al.* Experimental and theoretical comparison of actinide and lanthanide bonding in $M[N(EPR_2)_2]_3$ complexes (M = U, Pu, La, Ce; E = S, Se, Te; R = Ph, *i*Pr, H). *Inorg. Chem.* **47**, 29-41 (2007).

11. Ingram, K. I. M., Tassell, M. J., Gaunt, A. J. & Kaltsoyannis, N. Covalency in the f element-chalcogen bond. Computational studies of $M[N(EPR_2)_2]_3$ (M = La, Ce, Pr, Pm, Eu, U, Np, Pu, Am, Cm; E = O, S, Se, Te; R = H, ^{i}Pr, Ph). *Inorg. Chem.* **47**, 7824-7833 (2008).

12. Jones, M. B. *et al.* Uncovering f-element bonding differences and electronic structure in a series of 1 : 3 and 1 : 4 complexes with a diselenophosphinate ligand. *Chem. Sci.* **4**, 1189-1203 (2013).

13. Ephritikhine, M. The vitality of uranium molecular chemistry at the dawn of the XXIst century. *Dalton Trans.* 2501-2516 (2006).

14. Hayton, T. W. Metal-ligand multiple bonding in uranium: structure and reactivity. *Dalton Trans.* **39**, 1145-1158 (2010).

15. Hayton, T. W. Recent developments in actinide-ligand multiple bonding. *Chem. Commun.* **49**, 2956-2973 (2013).

16. Allen, F. H. The cambridge structural database: A quarter of a million crystal structures and rising. *Acta Cryst. Sect. B* **58**, 380 (2002).

17. Cantat, T. *et al.* The U=C double bond: synthesis and study of uranium nucleophilic carbene complexes. *J. Am. Chem. Soc.* **131**, 963-972 (2009).

18. Cooper, O. J. *et al.* Uranium-carbon multiple bonding: facile access to the pentavalent uranium carbene $[U\{C(PPh_2NSiMe_3)_2\}(Cl)_2(I)]$ and comparison of U^{V}=C and U^{IV}=C double bonds. *Angew. Chem. Int. Ed.* **50**, 2383-2386 (2011).

19. Tourneux, J. -C. *et al.* Exploring the uranyl organometallic chemistry: from single to double uranium-carbon bonds. *J. Am. Chem. Soc.* **133**, 6162-6165 (2011).

20. Fortier, S., Walensky, J. R., Wu, G. & Hayton, T. W. Synthesis of a phosphorano-stabilized U(IV)-carbene via one-electron oxidation of a U(III)-ylide adduct. *J. Am. Chem. Soc.* **133**, 6894-6897 (2011).

21. Mills, D. P. *et al.* Synthesis of a uranium(VI)-carbene: reductive formation of uranyl(V)-methanides, oxidative preparation of a $[R_2C=U=O]^{2+}$ analogue of the $[O=U=O]^{2+}$ uranyl ion (R = $Ph_2PNSiMe_3$), and comparison of the nature of U^{IV}=C, U^{V}=C and U^{VI}=C double bonds. *J. Am. Chem. Soc*. **134**, 10047-10054 (2012).

22. Lu, E. *et al*. Synthesis, characterization, and reactivity of a uranium(VI) carbene imido oxo complex. *Angew. Chem. Int. Ed.* **53**, 6696-6700 (2014).

23. Cramer, R. E., Panchanatheswaran, K. & Gilje, J. W. Uranium carbon multiple-bond chemistry. 3. Insertion of acetonitrile and the formation of a uranium nitrogen multiple bond *J. Am. Chem. Soc.* **106**, 1853-1854 (1984).

24. Brennan, J. G. & Andersen, R. A. Electron-transfer reactions of trivalent uranium. Preparation and structure of the uranium metallocene compounds $(MeC_5H_4)_3U$=NPh and $[(MeC_5H_4)_3U]_2[\mu\text{-}\eta^1,\eta^2\text{-PhNCO}]$. *J. Am. Chem. Soc.* **107**, 514-516 (1985).

25. Burns, C. J., Smith, W. H., Huffman, J. C. & Sattelberger, A. P. Uranium(VI) organoimido complexes. *J. Am. Chem. Soc.* **112**, 3237-3239 (1990).

26. Arney, D. S. J., Burns, C. J. & Smith, D. C. Synthesis and structure of the first uranium(VI) organometallic complex. *J. Am. Chem. Soc.* **114**, 10068-10069 (1992).

27. Arney, D. S. J. & Burns, C. J. Synthesis and properties of high-valent organouranium complexes containing terminal organoimido and oxo functional groups. A new class of organo-f-element complexes. *J. Am. Chem. Soc.* **117**, 9448-9460 (1995).

28. Hayton, T. W. *et al.* Synthesis of imido analogs of the uranyl ion. *Science* **310**, 1941 (2005).

29. Castro-Rodríguez, I., Nakai, H. & Meyer, K. Multiple-bond metathesis mediated by sterically pressured uranium complexes. *Angew. Chem. Int. Ed.* **45**, 2389-2392 (2006).

30. Graves, C. R. *et al.* Organometallic uranium(V)-imido halide complexes: from synthesis to electronic structure and bonding. *J. Am. Chem. Soc.* **130**, 5272-5285 (2008).

31. Bart, S. C. *et al*. Carbon dioxide activation with sterically pressured mid- and high-valent uranium complexes. *J. Am. Chem. Soc.* **130**, 12536-12546 (2008).

32. Matson, E. M., Crestani, M. G., Fanwick, P. E. & Bart, S. C. Synthesis of U(IV) imidos from $Tp^*_2U(CH_2Ph)$ (Tp* = hydrotris(3,5-dimethylpyrazolyl)borate) by extrusion of bibenzyl. *Dalton Trans.* **41**, 7952-7958 (2012).

33. Jilek, R. E. *et al*. A Direct Route to Bis(imido) uranium(V) Halides via Metathesis of Uranium Tetrachloride. *J. Am. Chem. Soc.* **134**, 9876-9878 (2012).

34. Camp, C., Pécaut, J. & Mazzanti, M. Tuning Uranium-Nitrogen Multiple Bond Formation with Ancillary Siloxide Ligands. *J. Am. Chem. Soc.* **135**, 12101-12111 (2013).

35. Lam, O. P. *et al.* Observation of the Inverse Trans Influence (ITI) in a Uranium(V) Imide Coordination Complex: An Experimental Study and Theoretical Evaluation. *Inorg. Chem.* **51**, 6190-6199 (2012).

36. Anderson, N. H. *et al*. Harnessing redox activity for the formation of uranium tris(imido) compounds. *Nat. Chem.* **6**, 919-926 (2014).

37. King, D. M. *et al.* Synthesis and characterization of an f-block terminal parent imido [U=NH] complex: a masked uranium(IV) nitride. *J. Am. Chem. Soc.* **136**, 5619-5622 (2014).

38. King, D. M. *et al*. Synthesis and structure of a terminal uranium nitride complex. *Science* **337**, 717-720 (2012).

39. King, D. M. *et al*. Isolation and characterization of a uranium(VI)-nitride triple bond. *Nat. Chem.* **5**, 482-488 (2013).

40. Cleaves, P. A. *et al*. Two-electron reductive carbonylation of terminal uranium(V) and uranium(VI) nitrides to cyanate by carbon monoxide. *Angew. Chem. Int. Ed.* **53**, 10412-10415 (2014).

41. Duttera, M. R., Day, V. W. & Marks, T. J. Organoactinide phosphine/phosphite coordination chemistry. Facile hydride-induced dealkoxylation and the formation of actinide phosphinidene complexes. *J. Am. Chem. Soc.* **106**, 2907-2912 (1984).

42. Arney, D. S. J., Schnabel, R. C., Scott, B. C. & Burns, C. J. Preparation of actinide phosphinidene complexes: steric control of reactivity. *J. Am. Chem. Soc.* **118**, 6780-6781 (1996).

43. Gardner, B. M. *et al.* Triamidoamine-uranium(IV)-stabilized terminal parent phosphide and phosphinidene complexes. *Angew. Chem. Int. Ed.* **53**, 4484-4488 (2014).

44. Brown, J. L., Fortier, S., Lewis, R. A., Wu, G. & Hayton, T. W. A complete family of terminal uranium chalcogenides, $[U(E)(N\{SiMe_3\}_2)_3]^-$ (E = O, S, Se, Te). *J. Am. Chem. Soc.* **134**, 15468-15475 (2012).

45. Brown, J. L., Fortier, S., Wu, G., Kaltsoyannis, N. & Hayton, T. W. Synthesis and spectroscopic and computational characterization of the chalcogenido-substituted analogues of the uranyl ion, $[OUE]^{2+}$ (E = S, Se). *J. Am. Chem. Soc.* **135**, 5352-5355 (2013).

46. Scherer, O. J., Werner, B., Heckmann, G. & Wolmershäuser. Bicyclic P_6 as Complex Ligand. *Angew. Chem. Int. Ed.* **30**, 553-555 (1991).

47. Stephens, F. H. PhD Thesis, Massachusetts Institute of Technology, 2004.

48. Frey, A. S. P., Cloke, F. G. N., Hitchcock, P. B. & Green, J. C. Activation of P_4 by $U(\eta^5\text{-}C_5Me_5)(\eta^8\text{-}C_8H_6(Si^iPr_3)_2\text{-}1,4)(THF)$; the X-ray structure of $[U(\eta^5\text{-}C_5Me_5)(\eta^8\text{-}C_8H_6(Si^iPr_3)_2\text{-}1,4)]_2(\mu\text{-}\eta^2\text{:}\eta^2\text{-}P_4)$. *New. J. Chem.* **35**, 2022-2026 (2011).

49. Patel, D. *et al.* An Actinide-Zintl Cluster: A Tris(Triamidouranium)$\mu_3\text{-}\eta^2\text{:}\eta^2\text{:}\eta^2$-Heptaphosphanortricyclane and its Diverse Synthetic Utility. *Angew. Chem. Int. Ed.* **52**, 13334-13337 (2013).

50. Selbin, J., Ahmad, N. & Pribble, M. J. Novel Complexes of Uranium(V). *J. Chem. Soc. Chem. Commun.* 759-760 (1969).

51. Deutscher, R. L. & Kepert, D. L. Eight-Coordinate Complexes of Niobium, Tantalum, and Uranium Tetrahalides. *Inorg. Chem.* **9**, 2305-2310 (1970).

52. Scherer, O. J., Schulze, J. & Wolmershäuser, G. Bicyclisches As_6 als komplexligand. *J. Organomet. Chem.* **484**, C5-C7 (1994).

53. Wu, Q. -Y. *et al*. Terminal U≡E (E = N, P, As, Sb, and Bi) Bonds in Uranium Complexes: A Theoretical Perspective. *J. Phys. Chem. A*, **119**, 922-930 (2015).

54. Andrews, L., Wang, X., Lindh, R., Roos, B. O., & Marsden, C. J. Simple N≡UF_3 and P≡UF_3 molecules with triple bonds to uranium. *Angew. Chem. Int. Ed.* **47**, 5366-5370 (2008).

55. Andrews, L., Wang, X. & Roos, B. O. As≡UF_3 molecule with a weak triple bond to uranium. *Inorg. Chem.* **48**, 6594-6598 (2009).

56. Ebsworth, E. A. V., Gould, R. O., Mayo, R. A. & Walkinshaw, M. Reactions of phosphine, arsine, and stibene with carbonylbis(triethylphosphine)iridium(I) halides. Part 1. Reactions in toluene; X-ray crystal; structures of [Ir(CO)ClH(PEt_3)$_2$(AsH_2)] and [Ir(CO)XH(PEt_3)$_2$(μ-ZH_2)$RuCl_2$(η^6-$MeC_6H_4CHMe_2$-*p*)] (X = Br, Z = P; X = Cl, Z = As). *J. Chem. Soc. Dalton. Trans* 2831-2838 (1987).

57. Becker, G. *et al*. Metal derivatives of molecular compounds. IX Bis(1,2-dimethoxyethane-*O*,*O*′)lithium phosphanide, arsanide, and chloride – three new representations of the Bis(1,2-dimethoxyethane-*O*,*O*′)lithium bromide type. *Z. Anorg. Allg. Chem.* **624**, 469-482 (1998).

58. Dixon, R. N., Duxbury, G. & Lamberton, H. M. Arsenic hydride radicals. *Chem. Commun. (London)* 460-461 (1966).

59. Herrmann, W. A., Koumbouris, B., Zahn, T. & Ziegler, M. L. Arsanediyl (Arsinidene) and diarsene complexes by metal-induced degradation of monoarsane. *Angew. Chem. Int. Ed. Engl.* **23**, 812-814 (1984).

60. Bachman, R. E., Miller, S. K. & Whitmire, K. H. Synthesis and structure of an anionic arsenic hydride complex: [PPN]$_2$[HAs{$Fe(CO)_4$}$_3$]•0.5THF. *Inorg. Chem.* **33**, 2075-2076 (1994).

61. Präsang, C., Stoelzel, M., Inoue, S., Meltzer, A. & Driess, M. Metal-free activation of EH_3 (E = P, As) by an ylide-like silylene and formation of a donor-stabilized arsasilene with a HSi=AsH subunit. *Angew. Chem. Int. Ed.* **49**, 10002-10005 (2010).

62. Johnson, B. P., Balázs, G. & Scheer, M. Low-coordinate E_1 ligand complexes of group 15 elements – a developing area. *Coord. Chem. Rev.* **250**, 1178-1195 (2006).

63. Spinney, H. A., Piro, N. A. & Cummins, C. C. Triple-bond reactivity of an AsP complex intermediate: synthesis stemming from molecular arsenic, As_4. *J. Am. Chem. Soc.* **131**, 16233-16243 (2009).

64. Curley, J. J., Piro, N. A. & Cummins, C. C. A terminal molybdenum arsenide complex synthesized from yellow arsenic. *Inorg. Chem.* **48**, 9599-9601 (2009).

65. Johnson, W. C. & Pechukas, A. Hydrogen compounds of arsenic. II. Sodium and potassium dihydrogen arsenides. *J. Am. Chem. Soc.* **59**, 2068-2071 (1937).

66. Peters, J. C., Odom, A. L. & Cummins, C. C. A terminal molybdenum carbide prepared by methylidyne deprotonation. *Chem. Commun.* 1995-1996 (1997).

67. Gardner, B. M. *et al.* The role of 5f-orbital participation in unexpected inversion of the σ-bond metathesis reactivity trend of triamidoamine thorium(IV) and uranium(IV) alkyls. *Chem. Sci.* **5**, 2489-2497 (2014).

68. Pyykkö, P. & Atsumi, M. Molecular single-bond covalent radii for elements 1-118. *Chem. Eur. J.* **15**, 186-197 (2009).

69. Pyykkö, P. & Atsumi, M. Molecular double-bond covalent radii for elements Li-E112. *Chem. Eur. J.* **15**, 12770-12779 (2009).

70. Pyykkö, P., Riedel, S. & Patzschke, M. Triple-bond covalent radii. *Chem. Eur. J.* **11**, 3511-3520 (2005).

71. Kindra, D. R. & Evans, W. J. Magnetic susceptibility of uranium complexes. *Chem. Rev*. **114**, 8865-8882 (2014).

72. Bader, R. F. W., Slee, T. S., Cremer, D. & Kraka, E. Descriptions of conjugation and hyperconjugation in terms of electron distributions. *J. Am. Chem. Soc.* **105**, 5061-5068 (1983).

73. Halter, D. P., La Pierre, H. S., Heinemann, F. W. & Meyer, K. Uranium(IV) halide (F^-, Cl^-, Br^-, and I^-) monoarene complexes. *Inorg. Chem.* **53**, 8418-8424 (2014).

74. Patel, D., McMaster, J., Lewis, W., Blake, A. J. & Liddle, S. T. Reductive assembly of cyclobutadienyl and diphosphacyclobutadienyl rings at uranium. *Nat. Commun*. **4**, 2323, doi:10.1038/ncomms3323 (2013).

Figures

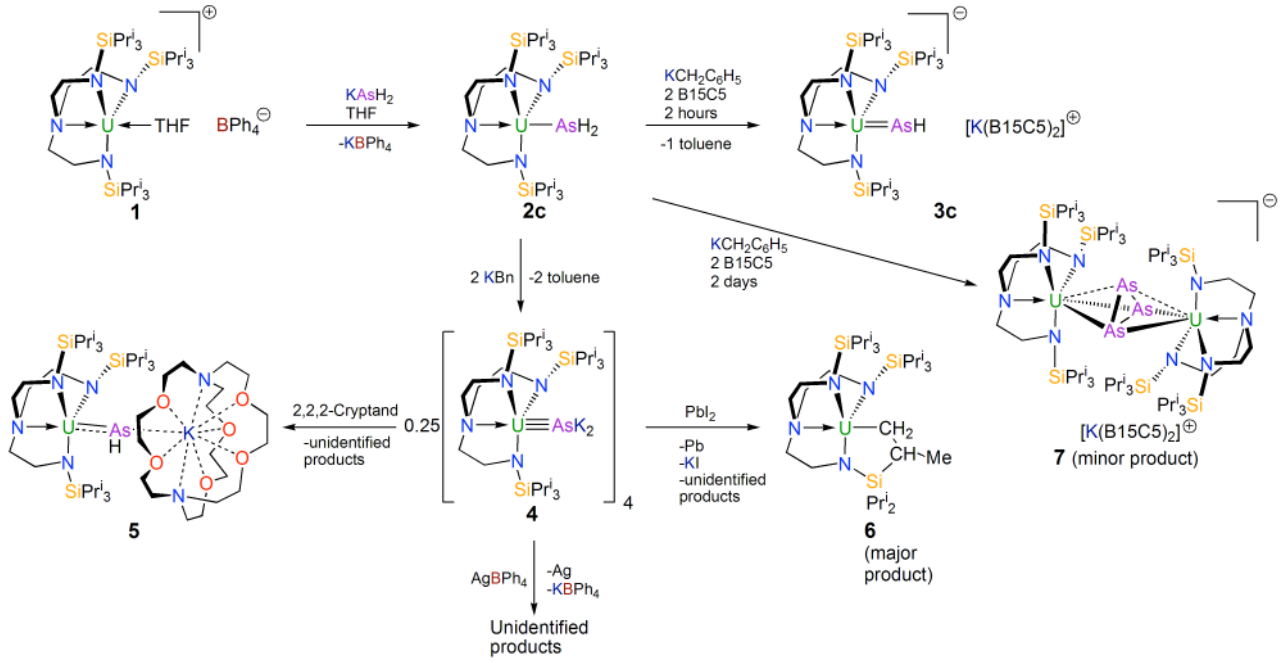

Figure 1. Synthesis of compounds 2c, 3c, 4, 5, 6, and 7 from precursor 1. Compound **1** reacts with $KAsH_2$ to give the uranium(IV) arsenide complex **2c** by salt elimination of $KBPh_4$. Single deprotonation of **2c** with benzyl potassium, followed by the addition of benzo-15-crown-5 ether, gives the separated ion pair parent terminal uranium(IV) arsinidene complex **3c**; if this reaction is left to stir for extended periods then decomposition occurs and only the diuranium(IV) triarsenide complex **7** can be isolated in very low yield. Double deprotonation of **2c** with benzyl potassium directly affords the tetrameric uranium(IV) arsenido complex **4**. Attempts to oxidize **4** with lead diiodide result in loss of the U-As linkage and formation of the known cyclometallate complex **6**. For the synthesis of **6** see Gardner and colleagues[67]. Treatment of **4** with $AgBPh_4$ resulted in decomposition to unidentified products, whereas treatment with 2,2,2-cryptand resulted in abstraction of a proton from solvent to afford the uranium(IV) arsinidiide complex **5** as well as unidentified products.

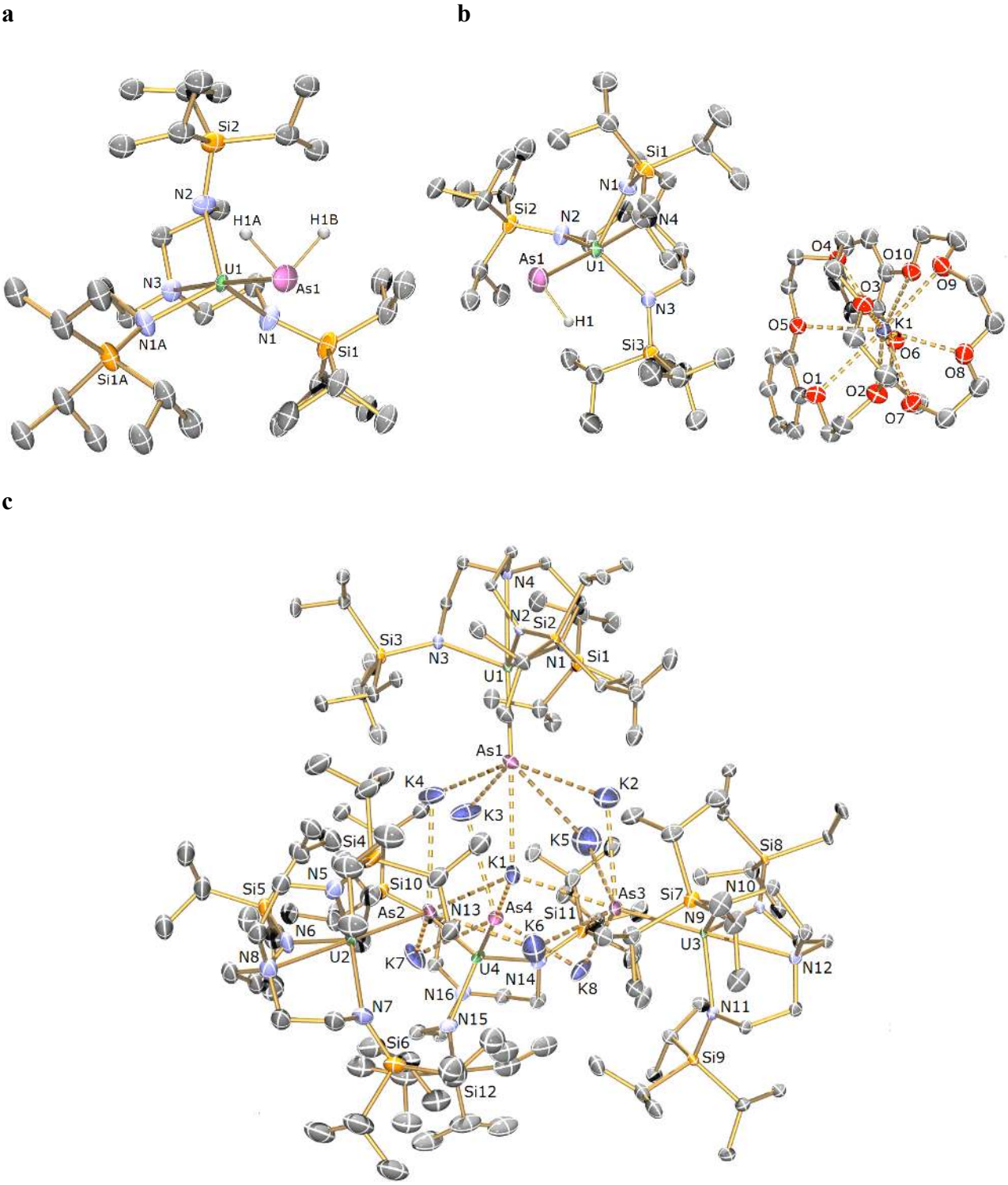

Figure 2. Molecular structures of 2c, 3c, and 4. **a-c**, solid state structures of **2c** (**a**), **3c** (**b**), **4** (**c**) by X-ray crystallography at 120 K with displacement ellipsoids set to 40% probability and hydrogen atoms, minor disorder components, and lattice solvent omitted for clarity. Green, uranium; purple, arsenic; dark blue, potassium; light blue, nitrogen; orange, silicon; gray, carbon; white, hydrogen.

a

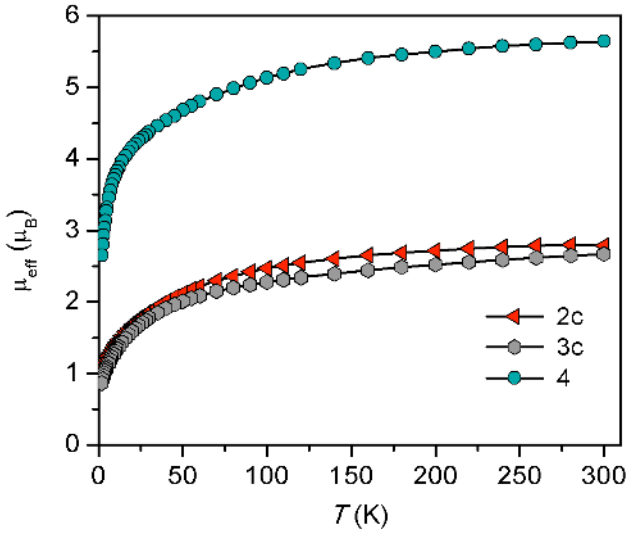

b

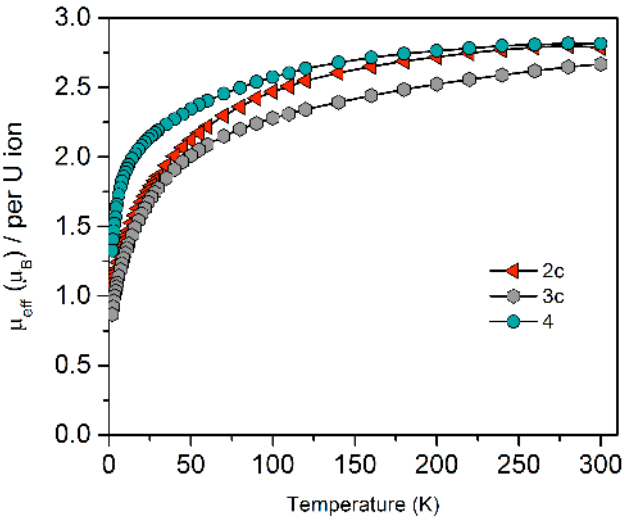

Figure 3. Variable temperature effective magnetic moment data for 2c, 3c, and 4. Data are plotted as μ_{eff} (μ_B) as a function of temperature (K) for **2c**, **3c** and **4** as powdered samples, measured by a superconducting quantum interference device (SQUID) magnetometer in an applied magnetic field of 0.1 T. **a**, magnetic moment per molecule. **b**, magnetic moment per uranium ion.

a **b** **c**

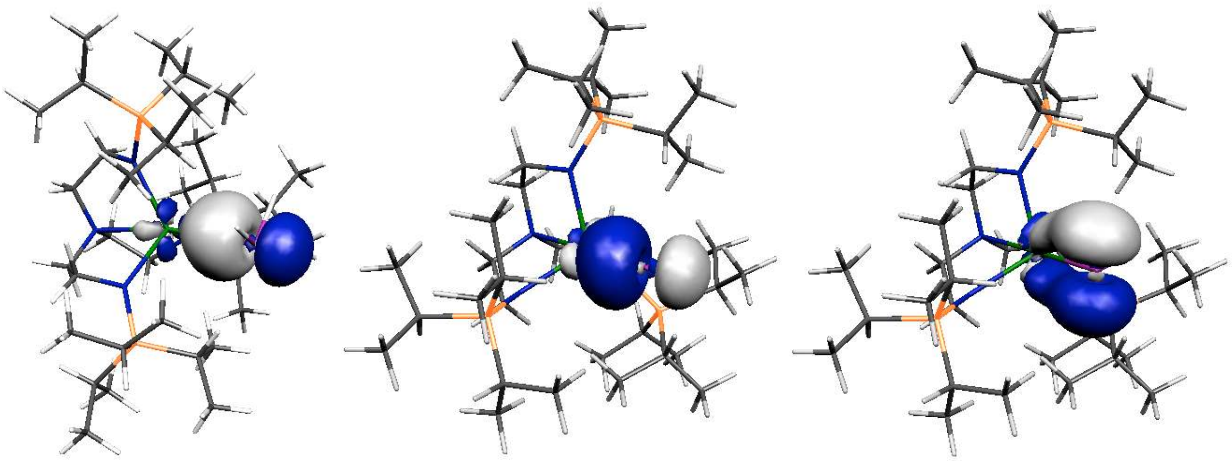

Figure 4. Selected NBOs that principally represent the U-As σ^2 and $\sigma^2\pi^2$ interactions in 2c and 3c. **a**, σ-bond in **2c**. **b**, σ-bond in **3c**. **c**, π-bond in **3c**. For the composition of these NBOs see Table 1. Green, uranium; purple, arsenic; blue, nitrogen; orange, silicon; gray, carbon; white, hydrogen.

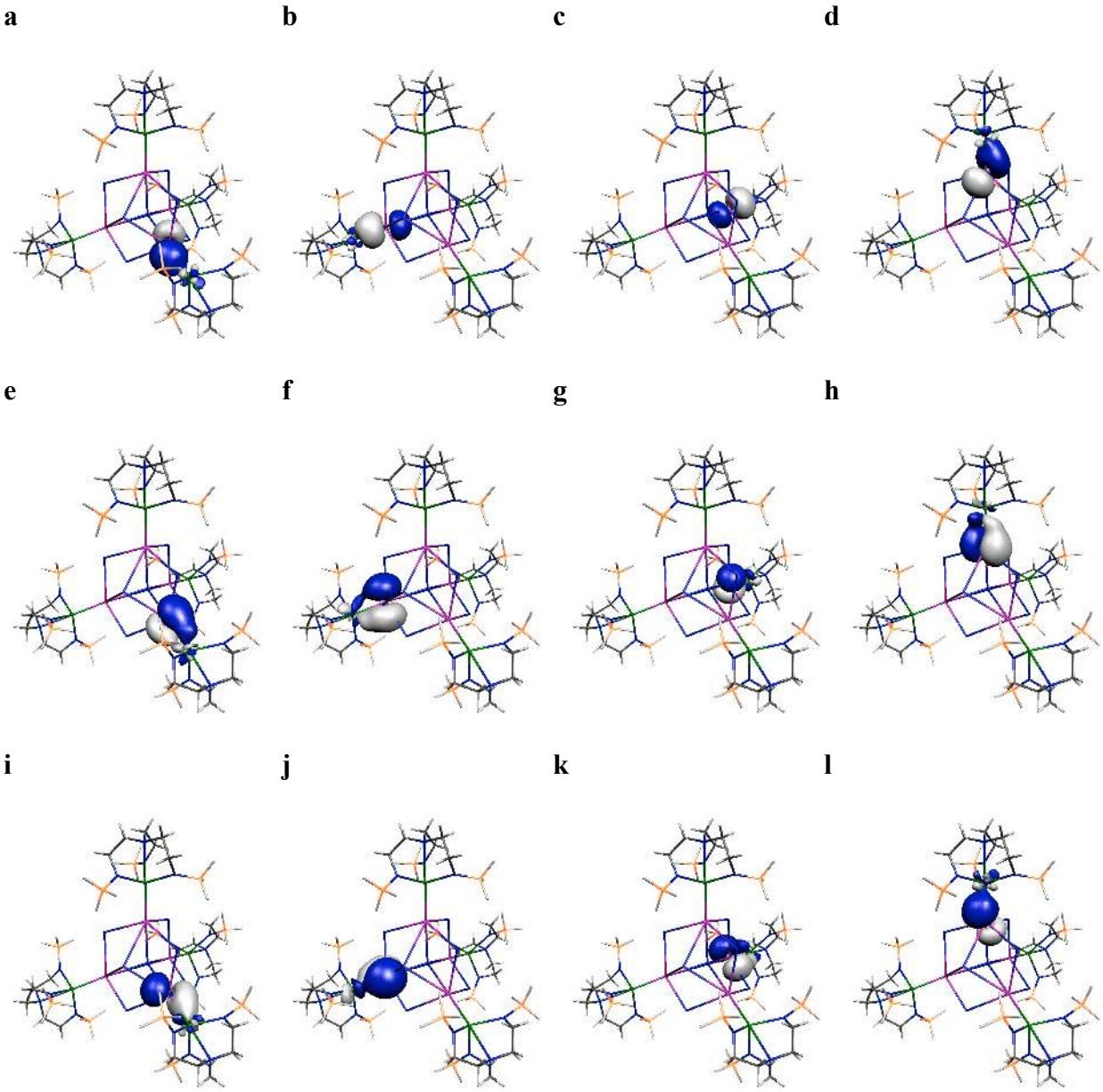

Figure 5. Selected NBOs that principally represent the four U-As $\sigma^2\pi^4$ interactions in the pruned model of 4'. **a-d** σ-bonds, **e-i** π-bonds. For the composition of these NBOs see Table 1. Green, uranium; purple, arsenic; dark blue, potassium; blue, nitrogen; orange, silicon; gray, carbon; white, hydrogen.

Table 1. Selected computed DFT and NBO data for **2c**, **3c**, and the pruned model of **4** (**4'**).

	Bond Lengths and Indices		Atomic Spin-Densities and Charges			NBO σ-component[g]			NBO π_1-component[g]			NBO π_2-component[g]		
Entry[a]	U-As[b]	BI[c]	m_U[d]	q_U[e]	q_{As}[f]	As%	U%	U 7s:7p:5f:6d	As%	U%	U 7s:7p:5f:6d	As%	U%	U 7s:7p:5f:6d
2c	3.0597	0.69	2.30	2.74	-0.51	86.7	13.3	3:2:48:47	-	-	-	-	-	-
3c	2.7537	1.62	2.32	2.50	-0.89	88.8	11.2	2:0:61:37	87.3	12.7	0:1:66:33	-	-	-
4'	2.7311	1.75	2.52	2.42	-1.66	82.9	17.1	2:1:57:40	80.8	19.2	0:1:69:30	83.8	16.2	0:1:55:44
	2.7426	1.48	2.49	2.53	-1.78	84.3	15.7	2:1:73:24	86.7	14.2	0:1:63:36	86.7	13.5	0:1:54:45
	2.7571	1.40	2.48	2.54	-1.82	85.6	14.4	2:1:70:27	85.8	13.3	0:1:62:37	86.5	13.3	0:1:65:34
	2.7741	1.38	2.25	2.59	-1.83	86.9	13.1	3:1:70:26	86.9	13.1	0:1:59:40	87.9	12.1	0:1:61:38

[a] All molecules geometry optimized without symmetry constraints using the BP86 GGA functional and a basis set derived from TZP/ZORA all-electron ADF database; all calculations were unrestricted. [b] Computational U-As distances (Å, not optimized for pruned model of **4**). [c] Mayer bond indices. [d] MDC-m α-spin densities on uranium. [e] MDC-q charges on uranium. [f] MDC-q charges on arsenic. [g] Natural Bond Orbital (NBO) analyses; the electron occupancies of these orbitals is ≥97%.